WorldCat 檢索項目: nb: 0784406464.

記錄 1 of 2

Designing, constructing, maintaining, and financing today's airport projects
proceedings of the twenty-seventh International Air Transport Conference, June 30-July 3, 2002, Orlando, Florida /

William J Sproule; Stacy Jansen

2002
英語 ◈ 圖書 電腦資料 1 v. (various pagings) : ill. (some col.) ; 22 cm.
Reston, Va. : American Society of Civil Engineers, ; ISBN: 0784406464 (CD-ROM)

取此文獻

館藏地點: **檢查貴圖書館的館藏**

- 世界各地擁有文獻的圖書館: 27
- Connect to the catalog at Tamkang University Library

查找相關文獻

其他類似記錄: 同題名和同著者版本 | 進階選項

有關: American Society of Civil Engineers. (201)

題名: **Designing, constructing, maintaining, and financing today's airport projects**
proceedings of the twenty-seventh International Air Transport Conference, June 30-July 3, 2002, Orlando, Florida /

著者: Sproule, William J. ; Jansen, Stacy.

Record 3 from Compendex for:(({Lee, Ying-Haur}) WN AU), 1969-2004

Check record to add to Selected Records

☑ 3. **Effects of Various Design Features on Rigid Airfield Pavement Design**

Lee, Ying-Haur (Department of Civil Engineering, Tamkang University); Yen, Shao-Tang **Source:** *Proceedings - International Air Transportation Conference*, 2002, p 77-91

CODEN: PIACDS

Conference: 27th International Air Transport Conference, Jun 30-Jul 3 2002, Orlando, FL, United States

Publisher: American Society of Civil Engineers

Abstract: Regardless of a shorter or longer joint spacing, a better or worse load transfer mechanism, and environmental effects, the required minimum slab thickness will be the same using the current airfield pavement design procedure. Thus, the primary objective of this study is to investigate the effects of many design features including finite slab sizes, thermal curling, moisture warping, and the presence of a second subbase layer on rigid airfield pavements in attempts to expand the applicability of the proposed thickness design procedure by Lee and Yen (2001). The Corps of Engineers full-scale test pavement data were reanalyzed. Several prediction models proposed by Lee, et al. (1997) were utilized to estimate the critical edge stress for design. Stress adjustment factors for finite slab width and length were determined and found to be negligible for the test data. Since the concept of transformed section was frequently utilized and sometimes misused in the literature to account for the stress reduction due to a bonded or unbonded second layer, a more complete treatment of this concept was presented. Subsequently, the stress adjustment factor was estimated assuming all subbase layers were unbonded. Climatic data close to the test track locations were obtained from the Long-Term Pavement Performance (LTPP) database and the stress adjustment factor due to effective temperature differentials was estimated. As a result, an alternative structural deterioration model was proposed for future trial analysis and design. The primary benefit of this study and recommendations for future implementation and investigations are discussed. (19 refs.)

Ei controlled terms: Airports | Pavements | Environmental impact | Structural design | Stresses | Poisson ratio | Elastic moduli | Computer software

Database: Compendex

Full-text and Local Holdings Links

SDOS | TKU Library

Effects of Various Design Features on Rigid Airfield Pavement Design

Ying-Haur Lee[1] and Shao-Tang Yen[2]

Abstract

Regardless of a shorter or longer joint spacing, a better or worse load transfer mechanism, and environmental effects, the required minimum slab thickness will be the same using the current airfield pavement design procedure. Thus, the primary objective of this study is to investigate the effects of many design features including finite slab sizes, thermal curling, moisture warping, and the presence of a second subbase layer on rigid airfield pavements in attempts to expand the applicability of the proposed thickness design procedure by Lee and Yen (*2001*).

The Corps of Engineers full-scale test pavement data were reanalyzed. Several prediction models proposed by Lee, *et al.* (*1997*) were utilized to estimate the critical edge stress for design. Stress adjustment factors for finite slab width and length were determined and found to be negligible for the test data. Since the concept of transformed section was frequently utilized and sometimes misused in the literature to account for the stress reduction due to a bonded or unbonded second layer, a more complete treatment of this concept was presented. Subsequently, the stress adjustment factor was estimated assuming all subbase layers were unbonded.

Climatic data close to the test track locations were obtained from the Long-Term Pavement Performance (LTPP) database and the stress adjustment factor due to effective temperature differentials was estimated. As a result, an alternative structural deterioration model was proposed for future trial analysis and design. The primary benefit of this study and recommendations for future implementation and investigations are discussed.

Introduction

The conventional Federal Aviation Administration's thickness design methodology (*FAA, 1995a*) for rigid airfield pavements was based on "the plate theory" and Westergaard's analytical solution for edge loading condition. In order to simplify the calculations, the critical edge loading stress was determined for an ideal infinite slab using Pickett and Ray's influence charts for some fixed aircraft gear

[1] Professor of Civil Engineering, Tamkang University, E725, #151 Ying-Chuan Rd., Tamsui, Taipei, Taiwan 251; phone 886-2-2623-2408; fax 886-2-2620-9747; yinghaur@mail.tku.edu.tw.

[2] Ph.D. Candidate, Department of Civil Engineering, Tamkang Univeristy, Taiwan.

configurations. The critical stress is also reduced by a factor of 25 percent to account for the effect of load transfer across the joints based on test results and past experiences and is still in use today. The effects of finite slab sizes, thermal curling, moisture warping, and the presence of a second subbase layer were accounted for through the fatigue curve developed by the Corps of Engineers from test track data and observation of full-scale test pavements. Nevertheless, these important design features are not part of the design procedure and the required slab thickness will be the same regardless of a shorter or longer joint spacing, a better or worse load transfer mechanism, other variations of wheel spacing and axle spacing, and environmental effects are considered.

Despite the fact that FAA (*1995b*) has adopted "the multi-layered linear elastic theory" for the design of both flexible and rigid airfield pavements to accommodate the new Boeing 777 airplanes, Lee and Yen (*2001*) proposed a new thickness design procedure for rigid airfield pavements particularly based on the conventional plate theory approach. The primary objective of this study is to address the continuous effort in the investigation of the effects of the aforementioned design features in rigid airfield pavement design.

Estimation of Critical Edge Stress for Design

The conventional FAA pavement design curves were developed using Westergaard edge loading analysis for rigid pavements. The critical edge stress (σ_e) was determined by:

$$\sigma_e = \frac{P}{h^2}\left[RC0 + RC1 \times \ln(\ell) + RC2 \times (\ln(\ell))^2\right] \quad (1)$$

Where RC0, RC1 and RC2 are the coefficients obtained using Pickett and Ray's influence charts for various aircraft types. P is the main landing gear load, lbs; σ_e is the critical edge tensile stress, psi; $\ell=(E*h^3/(12*(1-\mu^2)*k))^{0.25}$ is the radius of relative stiffness, in.; E is the elastic modulus of the slab, psi; k is the modulus of subgrade reaction, psi/in; μ is the Poisson's Ratio, and h or h_1 is the slab thickness, in.

Since equation (1) is only applicable to U.S. customary system and some fixed gear configurations, Lee and Yen (*2001*) proposed the following alternative equation, which is dimensionally correct, applicable to both U.S. customary system and metric system and various gear configurations:

$$\sigma_e = \sigma_{we} * R_1$$

$$\sigma_{we} = \frac{3(1+\mu)P}{\pi(3+\mu)h^2}\left[\ln\frac{Eh^3}{100ka^4} + 1.84 - \frac{4}{3}\mu + \frac{1-\mu}{2} + 1.18(1+2\mu)\frac{a}{\ell}\right] \quad (2)$$

Where, σ_e is the predicted critical edge stress, [FL^{-2}]; σ_{we} is the Westergaard's (*1948*) closed-form edge stress solution, [FL^{-2}]; P is main landing gear load, [F]; *a* is the applied load radius, [L]. R_1 is an adjustment (or multiplication) factor, which represents the combined effect of several prediction models for different gear

configurations including dual-wheel, tandem axle, and tridem axle.

To expand the applicability of the proposed thickness design procedure by Lee and Yen (*2001*) for different finite slab sizes, temperature curling, and the presence of a second subbase layer, the following equation proposed by Lee, *et al.* (*1997*) will be utilized in attempts to incorporate those important design features as part of the proposed thickness design approach for rigid airfield pavements:

$$\sigma_e = \sigma_{we} * R_1 * R_2 * R_5 + R_T * \sigma_c \tag{3}$$

Where, σ_c = Westergaard/Bradbury's curling stress, [FL^{-2}]; R_2 = adjustment factor for finite slab length and width; R_5 = adjustment factor for a bonded or unbonded second layer using the concept of transformed section; and R_T = adjustment factor for the combined effect of loading plus daytime curling.

Effect of Finite Slab Width and Length

The stress reduction effect of small slab sizes was always overlooked in the past and current rigid airfield pavement design approaches probably due to the fact that most rigid airfield pavements were built with very large slab sizes. It is noted, however, that the effect of finite slab sizes has been accounted for in the Portland Cement Association's (*PCA, 1984*) thickness design procedure for rigid highway pavements based on the results of J-SLAB finite element analysis.

Subsequently, the Corps of Engineers accelerated traffic data provided by Gucbilmez and Yuce (*1995*) and supplemental original pavement design information from the literature (*Parker, et al., 1979; U.S. Army Corps of Engineers, Waterways Experiment Station, 1974*) were obtained and reanalyzed in this study. As shown in Table 1, the stress adjustment factors (R_2) estimated in terms of R_W (ranging from 0.998 to 1.0) for finite slab width (W) and R_L (ranging from 0.964 to 1.0) for finite slab length (L) are indeed negligible for the full-scale test pavements.

Effect of a Second Subbase Layer

The subgrade k value was originally developed for characterizing the support of natural soils with fairly low shear strength. Substantially higher k values were obtained based on plate tests on the top of granular and stabilized base layers. The current and past FAA airfield pavement design approaches as well as the current PCA design procedure and the 1986 AASHTO Guide for concrete highway pavements all adopt the concept of a composite "top-of-the-base" k-value for design, though many researchers have indicated the inadequacy of this concept. Through the review of results from several field studies and the examination of the k-value methods introduced in the 1986 AASHTO Guide, "it is recommended that k values be selected for natural soil materials, and that base layers be considered in concrete pavement design in terms of their effect on the slab response, rather than their supposed effect on k value" (*Hall, et al, 1995; Darter, et al., 1995*). Improved guidelines for k-value selection from a variety of methods are provided in the 1998 Supplement Guide for the design of concrete pavement structures accordingly.

Even though the concept of transformed section was frequently utilized to account for the stress reduction factor (R_5) due to a bonded or unbonded second layer,

it was found to be sometimes misused in the literature (*Salsilli-Murua, 1991; Lee, et al., 1997; Kuo, 1994*). Subsequently, a more complete treatment of this concept is presented as follows.

Table 1. Effect of finite slab length and width.

Item	Q	h (cm)	k (MN/m^3)	E (GPa)	P (kN)	a (cm)	W (m)	L (m)	Sc (MPa)	R_W	R_L
A1.60	A	14.5	40.5	26.2	164.7	36.20	6.10	6.10	5.37	1.000	1.000
B2.66L	B	14.0	20.3	26.2	89.0	28.19	6.10	6.10	5.10	1.000	1.000
B1.66L	A	14.0	20.3	26.2	164.7	36.20	6.10	6.10	5.37	1.000	1.000
C2.66S	A	14.0	18.9	26.2	89.0	28.19	6.10	6.10	5.10	1.000	1.000
C1.66S	A	14.0	18.9	26.2	164.7	36.20	6.10	6.10	5.37	1.000	1.000
D1.66	A	14.0	20.3	26.2	164.7	36.20	6.10	6.10	5.37	1.000	1.000
E2.66M	B	14.6	28.1	26.2	89.0	28.19	6.10	6.10	5.10	1.000	1.000
E1.66M	A	14.6	28.1	26.2	164.7	36.20	6.10	6.10	5.37	1.000	1.000
F1.80	B	19.7	14.0	26.2	164.7	36.20	6.10	6.10	5.37	1.000	0.999
K2.100	B	24.0	24.3	26.2	267.0*	46.46	6.10	6.10	5.06	1.000	0.998
N1.86	A	20.3	20.3	26.2	164.7	36.20	6.10	6.10	5.37	1.000	0.999
N2.86	A	20.3	20.3	26.2	267.0	46.46	6.10	6.10	5.06	1.000	0.999
O1.106	A	24.0	20.3	26.2	164.7	36.20	6.10	6.10	5.37	1.000	0.992
O2.106	A	24.0	20.3	26.2	267.0	46.46	6.10	6.10	5.06	1.000	0.992
P1.812	A	19.3	25.7	26.2	164.7	36.20	6.10	6.10	5.37	1.000	0.997
P2.812	B	19.3	25.7	26.2	267.0	46.46	6.10	6.10	5.06	1.000	0.997
Q1.102	B	24.0	29.7	26.2	164.7	36.20	6.10	6.10	5.37	1.000	0.989
Q2.102	A	24.0	29.7	26.2	267.0	46.46	6.10	6.10	5.06	1.000	0.988
U1.60	A	14.8	55.9	26.2	164.7	36.20	6.10	6.10	5.37	1.000	1.000
E-6	A	51.5	26.2	27.6	667.5	54.74	7.62	7.62	4.82	1.000	0.964
M-1	A	30.5	14.9	28.4	667.5	47.09	7.62	7.62	5.00	0.999	0.997
M-2	A	38.1	14.9	28.4	667.5	47.09	7.62	7.62	5.00	1.000	0.987
-	B	15.2	16.7	27.6	267.0	36.93	3.05	7.62	5.51	1.000	1.000
59	B	40.6	12.7	29.6	445.0	27.71	7.62	15.24	5.03	1.000	1.000
60	B	30.5	90.5	29.6	445.0	27.71	7.62	15.24	5.03	1.000	1.000
61	B	35.6	81.0	29.6	445.0	27.71	7.62	15.24	5.03	0.999	1.000
62	B	40.6	97.2	29.6	445.0	27.71	7.62	15.24	5.03	0.999	1.000
72	B	71.1	18.9	28.9	1446.3	49.96	15.24	15.24	5.51	0.999	1.000
73	A	61.0	18.9	28.9	1446.3	49.96	15.24	15.24	5.51	0.998	1.000
1-C5	A	25.4	13.5	41.3	1602.0	83.79	7.62	7.62	5.00	0.999	0.998
2-DT	A	30.5	18.9	41.3	738.7	41.22	7.62	7.62	4.82	0.999	0.996
3-DT	A	35.6	20.0	41.3	738.7	41.22	7.62	7.62	4.55	0.999	0.990
2-C5	A	27.9	27.0	41.3	1602.0	83.79	7.62	7.62	5.03	0.999	1.000
4-DT	A	25.4	63.5	41.3	738.7	41.22	7.62	7.62	5.93	0.999	1.000
3-200	A	38.1	27.5	41.3	890.0	46.84	7.62	7.62	6.20	0.999	0.987
4-200	A	38.1	33.8	41.3	890.0	46.84	7.62	7.62	5.99	0.999	0.987

Note: Item name is the same item designation used by Gucbilmez and Yuce (1995). Assuming μ=0.2. In which, S_c is the concrete flexural strength; R_w and R_L are the effects of finite slab width (W) and length (L), respectively. * denotes the main landing gear load (P) of Item K2.100 was originally mistyped by Gucbilmez and Yuce (1995) and thus subsequently corrected in this study.

Stress Adjustment due to a Second Unbonded Subbase Layer

Following the formulation given by Tabatabai-Raissi (*1977*), a system of two unbonded layers is transformed into an equivalent single layer based on the assumption of same total bending moment as shown in Figure 1. The maximum bending moment per unit of width of a given single layer is equal to$\sigma h^2/6$. Assuming both layers have the same Poisson's ratio ($\mu_1=\mu_2$), the relationship of the top layer stress (σ_1) and the bottom layer stress (σ_2), the total bending moment per unit of width (M_T) and the effective thickness (h_{eff}) can be expressed by:

$$\frac{\sigma_1}{\sigma_2}=\frac{E_1 h_1}{E_2 h_2} \tag{4}$$

$$M_T=\frac{\sigma_1}{6}\left[h_1^{\,2}+\left(\frac{E_2 h_2}{E_1 h_1}\right)h_2^{\,2}\right]=\frac{\sigma_1 h_{eff}^2}{6} \tag{5}$$

$$h_{eff}=\sqrt{h_1^{\,2}+\left(\frac{E_2 h_2}{E_1 h_1}\right)h_2^{\,2}} \tag{6}$$

In which, E_1, E_2= modulus of elasticity of the slab and subbase layers; and h_1, h_2= thickness of the slab and subbase layers, respectively.

(a) single layer (b) two unbonded layers (c) equivalent single layer

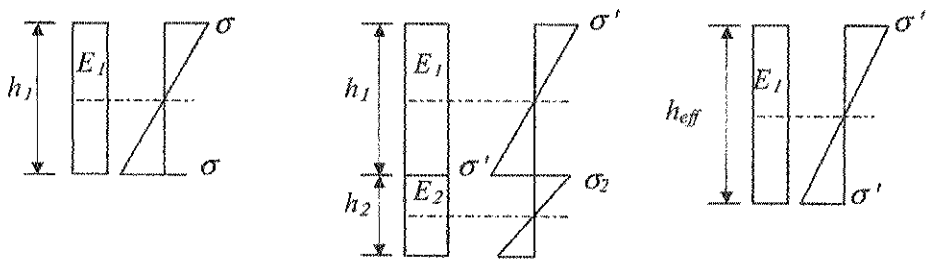

Figure 1. Transforming two unbonded layers into an equivalent single layer.

Alternatively, using equivalent moment of inertia per unit of width (I_{eff}) for the transformed section with modulus E_1, the effective thickness (h_{eff}) and the slab bending stress (σ_{unbond}) of the two-layer unbonded system can be determined by:

$$I_{eff}=I_1+\left(\frac{E_2}{E_1}\right)I_2=\frac{h_1^{\,3}}{12}+\left(\frac{E_2}{E_1}\right)\frac{h_2^{\,3}}{12}=\frac{h_{eff}^{\,3}}{12}$$

$$h_{eff}=\sqrt[3]{h_1^{\,3}+\left(\frac{E_2}{E_1}\right)h_2^{\,3}} \tag{7}$$

$$\sigma_{unbond} = \sigma_{we} \times \frac{h_1}{h_{eff}} \times \frac{\sigma'}{\sigma} = \sigma_{we} \times R_s \tag{8}$$

In which, σ and σ' are the slab bending stress of a single layer and the equivalent single layer to be determined by equation (2), respectively. Also note that the multiplication factor of h_1/h_{eff} is necessary to adjust the stress proportionally according to Figure 1 (b) and (c).

Stress Adjustment due to a Second Bonded Subbase Layer

As for the case of two bonded layers, considering a cross section of the slab/subbase system as an equivalent single layer, its corresponding strain and stress relationships are shown in Figure 2. The location of the neutral axis is defined at a distance x from the bottom of the second layer:

$$x = \frac{E_1 h_1^2 + 2E_1 h_1 h_2 + E_2 h_2^2}{2(E_1 h_1 + E_2 h_2)} \tag{9}$$

In which, α and β are the distances of the neutral axis from the middle surfaces of the second layer and the top layer, respectively ($\alpha = x - h_2/2$, $\beta = h_2 + h_1/2 - x$).

(a) two bonded layers (b) Strain (c) Stress

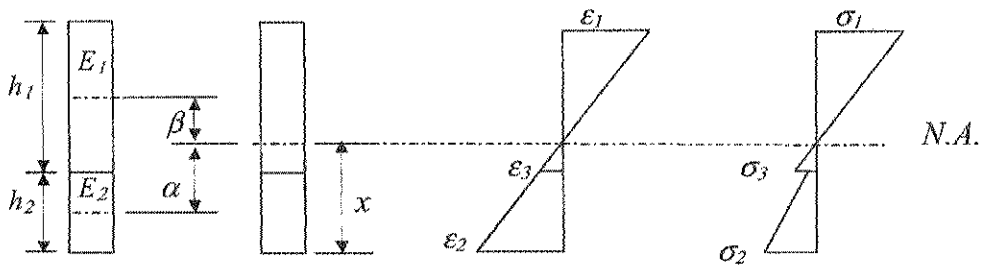

Figure 2. Considering two bonded layers as an equivalent single layer.

By converting this system into an equivalent unbonded system as shown in Figure 3, the equivalent top layer thickness (h_{1f}) and bottom layer thickness (h_{2f}) become $h_{1f} = \sqrt[3]{h_1^3 + 12h_1\beta^2}$ and $h_{2f} = \sqrt[3]{h_2^3 + 12h_2\alpha^2}$. Similarly, using the equivalent moment of inertia per unit of width (I_{eff}) for the transformed section with modulus E_1, the effective thickness (h_{eff}) and the slab bending stress (σ_{bond}) of the two-layer bonded system can be determined by the following expression:

$$h_{eff} = \sqrt[3]{h_{1f}^3 + \left(\frac{E_2}{E_1}\right) h_{2f}^3} \tag{10}$$

$$\sigma_{bond} = \sigma_{we} \times \frac{2(x - h_2)}{h_{eff}} \times \frac{\sigma'}{\sigma} = \sigma_{we} \times R_5 \qquad (11)$$

In which, σ and σ' are the slab bending stress of a single layer and the equivalent single layer to be determined by equation (2), respectively. Also note that the multiplication factor of $2(x\text{-}h_2)/h_{eff}$ is necessary to adjust the stress proportionally according to Figure 3 (a) and (b).

Furthermore, the applicability of the stress adjustment equations (8) and (11) was verified through comparison of the results of a series of ILLI-SLAB finite element runs and the ILLICON program (*NCHRP, 1990*) with excellent agreements.

(a) converting into two unbonded layers (b) Stress

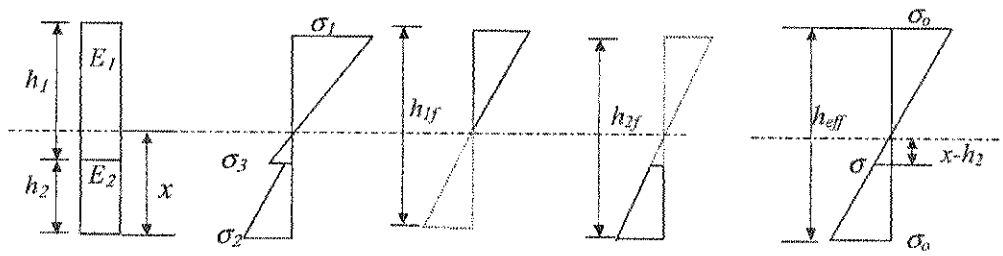

Figure 3. Transforming two bonded layers into two unbonded layers.

Reanalysis Results: Assuming a Second Unbonded Subbase Layer

As shown in Table 2, the Corps of Engineers accelerated traffic data was reanalyzed in this study (*Gucbilmez and Yuce, 1995; Parker, et al., 1979; U.S. Army Corps of Engineers, Waterways Experiment Station, 1974*). Since there existed some discrepancies in the subgrade modulus (k) obtained from Gucbilmez and Yuce (*1995*) against the original pavement design information, a stress adjustment factor (R_k) (ranging from 1.00 to 1.248) was introduced to illustrate the difference using two sets of k values. By assuming all second subbase layers were unbonded while using the new set of k values, the stress adjustment factor (R_5) (ranging from 0.987 to 1.0) was estimated for the full-scale test pavements.

Effect of Thermal Curling and Moisture Warping

A daytime positive temperature differential through the slab thickness induces additional tensile stresses at the bottom of the slab, whereas higher moisture content generally exists at the bottom of the slab during daytime non-raining periods, additional compressive stresses will occur at the bottom of the slab. Even though the effects of thermal curling and moisture warping may result in very different critical tensile stresses and thus cumulative fatigue damage, their effects were embedded in the fatigue curve developed by the Corps of Engineers from the full-scale test track data. Thermal and moisture gradients highly depend on a variety of factors such as air temperature, the ambient relative humidity at the slab surface, free water in the

slab, and the moisture content of the subbase or subgrade, which are very difficult to measure accurately. Thus, these important design features are not part of the past and current airfield pavement design procedures.

Table 2. Effect of subgrade modulus discrepancy and a second unbonded layer.

Item	Q	h_1 (cm)	E_1 (GPa)	h_2 (cm)	E_2 (GPa)	k* (MN/m^3)	k (MN/m^3)	R_k	R_5
A1.60	A	14.5	26.2	0.0	0.000	40.5	40.5	1.000	1.000
B2.66L	B	14.0	26.2	0.0	0.000	20.3	20.3	1.000	1.000
B1.66L	A	14.0	26.2	0.0	0.000	20.3	20.3	1.000	1.000
C2.66S	A	14.0	26.2	15.2	0.041	18.9	18.9	1.000	0.998
C1.66S	A	14.0	26.2	15.2	0.041	18.9	18.9	1.000	0.998
D1.66	A	14.0	26.2	15.2	0.069	20.3	16.2	1.069	0.997
E2.66M	B	14.6	26.2	15.2	0.124	28.1	19.2	1.100	0.996
E1.66M	A	14.6	26.2	15.2	0.124	28.1	19.2	1.128	0.996
F1.80	B	19.7	26.2	0.0	0.000	14.1	14.0	1.000	1.000
K2.100	B	24.0	26.2	0.0	0.000	24.3	24.3	1.000	1.000
N1.86	A	20.3	26.2	15.2	0.069	20.3	16.2	1.045	0.999
N2.86	A	20.3	26.2	15.2	0.069	20.3	16.2	1.053	0.999
O1.106	A	24.0	26.2	15.2	0.069	20.3	16.2	1.040	0.999
O2.106	A	24.0	26.2	15.2	0.069	20.3	16.2	1.045	0.999
P1.812	A	19.3	26.2	30.5	0.103	25.7	11.6	1.179	0.987
P2.812	B	19.3	26.2	30.5	0.103	25.7	11.6	1.210	0.988
Q1.102	B	24.0	26.2	30.5	0.103	29.5	13.5	1.153	0.993
Q2.102	A	24.0	26.2	30.5	0.103	29.5	13.5	1.176	0.994
U1.60	A	14.8	26.2	0.0	0.000	55.9	55.9	1.000	1.000
E-6	A	51.5	27.6	0.0	0.000	26.2	26.2	1.000	1.000
M-1	A	30.5	28.4	0.0	0.000	14.9	14.9	1.000	1.000
M-2	A	38.1	28.4	0.0	0.000	14.9	14.9	1.000	1.000
-	B	15.2	27.6	0.0	0.000	16.8	16.7	1.000	1.000
59	B	40.6	29.6	0.0	0.000	12.7	12.7	1.000	1.000
60	B	30.5	29.6	0.0	0.000	90.5	90.5	1.000	1.000
61	B	35.6	29.6	0.0	0.000	81.1	81.0	1.000	1.000
62	B	40.6	29.6	0.0	0.000	97.3	97.2	1.000	1.000
72	B	71.1	28.9	0.0	0.000	18.9	18.9	1.000	1.000
73	A	61.0	28.9	0.0	0.000	18.9	18.9	1.000	1.000
1-C5	A	25.4	41.3	0.0	0.000	16.2	13.5	1.042	1.000
2-DT	A	30.5	41.3	0.0	0.000	18.9	18.9	1.000	1.000
3-DT	A	35.6	41.3	0.0	0.000	20.0	20.0	1.000	1.000
2-C5	A	27.9	41.3	0.0	0.000	27.0	27.0	1.000	1.000
4-DT	A	25.4	41.3	15.2	1.723	63.5	22.2**	1.248	0.992
3-200	A	38.1	41.3	15.2	1.378	27.6	22.2**	1.055	0.998
4-200	A	38.1	41.3	15.2	1.378	33.8	22.2**	1.111	0.998

Note: Item name is the same item designation used by Gucbilmez and Yuce (1995). In which, * denotes the subgrade modulus (k) was obtained from the above literature; ** denotes the subgrade modulus (k) was estimated from $k = (E_{sg}/26)^{0.7788}$, suggested by PCA and WES-TR-GL-79-4. Both k (pci) and E_{sg} (psi) are in US customary system (1 pci = 0.27 MN/m^3 and 1psi = 6.89 kPa).

On the other hand, based on practical considerations of the difficulty and variability in determining temperature differentials, the 1998 AASHTO Supplement to the Guide for Design of Pavement Structures (*1998*) has incorporated the concept of effective temperature differential (*Kuo, 1998*). Field temperature measurements during different times of a day at 14 sites in the US were input to calculate pavement compound stresses due to curling and loading using three-dimensional finite-element analysis. Effective temperature differential were determined based on equivalent fatigue damages for highway pavements. The relationship between daytime effective temperature differential and climatic factors was derived by:

$$TD = 0.962 - \frac{52.181}{h} + 0.341 * WIND + 0.184 * TEMP - 0.00836 * PREC \qquad (12)$$

Where, TD = effective positive temperature differential, °F; h = slab thickness, in.; WIND = mean annual wind speed, mph; TEMP = mean annual temperature, °F; and PREC = mean annual precipitation, in. The summary statistics are: $R^2 = 0.84$, N = 42, SEE = 1.2 °F. (1 °C = 1.8 °F, 2.54 cm = 1 in.; 1 m/s = 2.24 mph)

In attempts to separate these effects from the fatigue relationship developed earlier, climatic data close to the Corps of Engineers accelerated test track locations were obtained from the Long-Term Pavement Performance (LTPP) database. These include Zone1 (Lockbourne Air Force Base, Ohio), Zone2 (Sharonville, Ohio) and Zone3 (Waterways Experiment Station, Mississippi). As shown in Table 3, effective positive temperature differential was estimated using equation (12). The critical edge stress due to loading (σ_L) alone was estimated, which is equivalent to the product of σ_{we}, R_1, R_W, R_L, and R_5. Additionally, the stress adjustment factor (R_{TD}) defined as the ratio of estimated combined loading plus curling stress (σ_e) given in equation (3) and loading stress (σ_L) was also estimated for the full-scale test pavements. Note that the estimated R_{TD} range is from 1.0 to 1.241.

Fatigue Relationship and Thickness Design Criteria

The conventional FAA thickness design methodology was based on an earlier fatigue curve developed by the Corps of Engineers from test track data and observation of full-scale test pavements. The fatigue curve originally adopted a bilinear relationship between a design factor (DF) and the number of load repetitions (in terms of coverages, C) at the specified failure criteria. The design factor (DF) is defined as the ratio of concrete flexural strength (S_c) to the allowable slab tensile stress (σ_a = 0.75 * σ_e). Rollings and Witczak (*1990*) developed a structural deterioration model for rigid airfield pavements that predicts performance in terms of a structural condition index (SCI) using multi-layered elastic pavement model. The SCI is derived from the pavement condition index (PCI) considering the distresses associated with tensile fatigue loading only and is on a scale from 0 to 100. The SCI is defined by $SCI = 100 \times \log(CF/C)/\log(CF/CO)$, in which CO is the coverages at the onset of structural deterioration; CF is the coverages at absolute failure; and C is the coverages at which SCI is to be calculated. Failure is defined as the number of coverages (C_{80}) to reduce the SCI from 100 to 80 at any given value of design factor.

Table 3. Effect of thermal curling and moisture warping.

Item	Q	Zone	h (cm)	PRECIP (mm)	TEMP (°C)	WIND (m/s)	TD (°C)	σ_L (MPa)	R_{TD}
A1.60	A	1	14.5	983.0	11.3	3.21	1.99	8.57	1.035
B2.66L	B	1	14.0	983.0	11.3	3.21	1.79	7.34	1.035
B1.66L	A	1	14.0	983.0	11.3	3.21	1.79	10.64	1.024
C2.66S	A	1	14.0	983.0	11.3	3.21	1.79	7.45	1.035
C1.66S	A	1	14.0	983.0	11.3	3.21	1.79	10.85	1.024
D1.66	A	1	14.0	983.0	11.3	3.21	1.79	11.35	1.023
E2.66M	B	1	14.6	983.0	11.3	3.21	2.02	6.99	1.042
E1.66M	A	1	14.6	983.0	11.3	3.21	2.02	10.26	1.029
F1.80	B	1	19.7	983.0	11.3	3.21	3.32	7.53	1.059
K2.100	B	1	24.0	983.0	11.3	3.21	3.99	8.29 *	1.065
N1.86	A	1	20.3	983.0	11.3	3.21	3.44	7.00	1.067
N2.86	A	1	20.3	983.0	11.3	3.21	3.44	9.35	1.050
O1.106	A	1	24.0	983.0	11.3	3.21	3.99	5.44	1.090
O2.106	A	1	24.0	983.0	11.3	3.21	3.99	7.37	1.067
P1.812	A	1	19.3	983.0	11.3	3.21	3.23	7.94	1.052
P2.812	B	1	19.3	983.0	11.3	3.21	3.23	10.66	1.039
Q1.102	B	1	24.0	983.0	11.3	3.21	3.99	5.58	1.083
Q2.102	A	1	24.0	983.0	11.3	3.21	3.99	7.58	1.062
U1.60	A	1	14.8	983.0	11.3	3.21	2.09	7.49	1.043
E-6	A	1	51.5	983.0	11.3	3.21	5.63	4.54	1.152
M-1	A	1	30.5	983.0	11.3	3.21	4.64	6.10	1.085
M-2	A	1	38.1	983.0	11.3	3.21	5.13	4.51	1.105
-	B	1	15.2	983.0	11.3	3.21	2.23	12.27	1.028
59	B	2	40.6	1066.2	11.2	4.05	5.58	5.60	1.154
60	B	2	30.5	1066.2	11.2	4.05	4.97	5.98	1.145
61	B	2	35.6	1066.2	11.2	4.05	5.32	4.93	1.186
62	B	2	40.6	1066.2	11.2	4.05	5.58	3.94	1.241
72	B	2	71.1	1066.2	11.2	4.05	6.35	4.00	1.212
73	A	2	61.0	1066.2	11.2	4.05	6.18	4.98	1.138
1-C5	A	3	25.4	1441.9	17.6	3.08	5.19	7.48	1.117
2-DT	A	3	30.5	1441.9	17.6	3.08	5.68	6.90	1.127
3-DT	A	3	35.6	1441.9	17.6	3.08	6.02	5.54	1.149
2-C5	A	3	27.9	1441.9	17.6	3.08	5.46	5.65	1.187
4-DT	A	3	25.4	1441.9	17.6	3.08	5.19	8.41	1.118
3-200	A	3	38.1	1441.9	17.6	3.08	6.16	5.67	1.148
4-200	A	3	38.1	1441.9	17.6	3.08	6.16	5.67	1.148

Note: Item name is the same item designation used by Gucbilmez and Yuce (1995). Zone1 - Lockbourne Air Force Base, Ohio; Zone2 - Sharonville, Ohio; Zone3- Waterways Experiment Station, Mississippi. The climatic data were estimated from the Long-Term Pavement Performance (LTPP) database. * denotes the critical load stress (σ_L) was greatly influenced by the correction of the main landing gear load (P) for Item K2.100 as indicated in Table 1.

Gucbilmez and Yuce (*1995*) later reanalyzed the Corps of Engineers accelerated traffic data and provided an alternative rigid airfield pavement deterioration relationship using stresses calculated by the Westergaard edge loading idealization. Lee and Yen (*2001*) further identified the shortcoming of the pass-to-coverage (P/C) concept, which implies that maximum tensile stress should be used throughout when the centerline location of the lateral wheel load placement (L_c) falls within the tire print area. In other words, the well-recognized effect of stress reduction due to the wandering of the L_c, moving away from the maximum tensile stress location, is totally neglected using the P/C concept. Consequently, an equivalent design factor (EDF) is defined by EDF = S_c / (0.75 * σ_e * f_3) to account for the reduction of critical edge stress due to the load location moving away from the slab edge. As a result, the following alternative fatigue relationship was proposed:

$$SCI = \frac{100*\log(C) - 324.044(EDF) + 119.799}{0.184217(EDF) - 1.00098}$$
$$EDF = 0.5900 + 0.2952*\log(C_{80}) \qquad (13)$$
$$DF = f_3*[0.5900 + 0.2952*\log(C_{80})]$$

The concept of "cumulative damage factor" (CDF) using Miner's hypothesis adopted in the LEDFAA thickness design approach was utilized as the fatigue failure criteria. CDF is the amount of the consumed structural fatigue life and is expressed as the summation of the ratio of applied load repetitions to allowable load repetitions to failure. When the damaging effects of all aircraft sums to 1.0, the design conditions have been satisfied and the required slab thickness is determined.

Alternative Structural Deterioration Relationship

Since the coverages at failure obtained from the fatigue curves were implicitly tied to the manner in which critical tensile stress was determined. With the effects of many design features (in terms of stress adjustment factors) being separately determined earlier, it is possible to incorporate them as part of the thickness design procedure, providing that an alternative structural deterioration relationship be developed based on critical edge stresses determined by the proposed equation (3).

Similarly, the P/C ratio and the f_3 value of each original test item of the Corps of Engineers test pavements were calculated according to the literature (*Lee and Yen, 2001*). Equivalent design factor (EDF) was defined the same as before with the only exception that the critical edge stress (σ_e) was determined by equation (3). In other words, σ_e is equivalent to the product of σ_{we}, R_1, R_W, R_L, R_5, and R_{TD} in this study. Fatigue relationships were developed for CO, CI and CF as functions of EDF and are listed as models #1 to #3 in Table 4. In addition, models #4 to #6 are developed for the passes at the onset of structural deterioration (PO), at initial failure (PI), and at absolute failure (PF) as functions of DF in case of future possible dismissal of the P/C concept.

Consequently, by solving models #1 and #3 for CO and CF and then substituting them into the SCI equation defined by Gucbilmez and Yuce (*1995*), the following alternative fatigue relationship was obtained:

$$SCI = \frac{100*\log(C) - 372.439(EDF) + 131.099}{0.3291(EDF) - 1.1373}$$
$$EDF = 0.5569 + 0.2508*\log(C_{80}) \quad (14)$$
$$DF = f_3*[0.5569 + 0.2508*\log(C_{80})]$$

Table 4. Alternative structural deterioration relationships.

Model No.	Tentative Fatigue Equations	SEE	R^2	N
#1	EDF = 0.6040 + 0.2467*log(CO)	0.115	0.742	24
#2	EDF = 0.5082 + 0.2493*log(CI)	0.113	0.788	36
#3	EDF = 0.3520 + 0.2685*log(CF)	0.118	0.730	24
#4	EDF = 0.4910 + 0.2422*log(PO)	0.121	0.716	24
#5	EDF = 0.3975 + 0.2441*log(PI)	0.118	0.769	36
#6	EDF = 0.2354 + 0.2629*log(PF)	0.124	0.701	24
#2*	EDF = 0.4719 + 0.2680*log(CI)	0.101	0.838	35
#5*	EDF = 0.3542 + 0.2619*log(PI)	0.107	0.816	35

Note: CO = the coverages at the onset of structural deterioration; CI = the coverages at initial failure (CI); and CF = the coverages at absolute failure. * stands for the models were developed without the possible outlying item 59. SEE is the standard error of estimate, R^2 is the coefficient of determination, and N is the number of observations.

Discussion and Implementation of the Proposed Approach

In order to isolate the effects of many design features embedded in the earlier fatigue curves developed from the Corps of Engineers full-scale test pavements, several necessary approximations and assumptions were made in conducting the analysis. The relationships among DF, EDF, and CO, CI, CF or PO, PI, PF are generally in relatively good agreement with those in the original models (*Lee and Yen, 2001*). Preliminary analysis by scatter plots also verified the overall trends were unchanged with slightly increasing variability. Originally, two possible outlying items (K2.100 and 59) were identified for the relationship of EDF versus CI and PI. In which, the main landing gear load (P) of Item K2.100 was later found to be mistyped in the literature and thus subsequently corrected throughout this study. As shown in Table 4, it may be possible to improve the summary statistics by excluding the other Item 59 from the models #2* and #5*, for example, if enough supporting evidences are further identified.

The primary benefit of developing the alternative fatigue curve (equation 14) based on its more realistically critical edge stresses is to expand its applicability for future trial analysis in incorporating many new design features as part of the thickness design procedure. Thus, newly innovative designs with the consideration of different finite slab sizes, local climatic effects (in terms of effective temperature differentials), as well as the presence of a second bonded / unbonded subbase layer,

which might not exist in the full-scale test items, may be possible.

For example, a sensitivity analysis of the effect of a second bonded or unbonded subbase layer on critical edge stress reduction was conducted as shown in Table 5. Based on the results of this comparison, the stress reduction factor (R_5) of an unbonded layer with low modulus (e.g., E_2 = 0.17 GPa) is negligible whereas the stress reduction factor of a second layer with high modulus (e.g., E_2 = 13.78 GPa) is more pronounced for the bonded cases.

The proposed stress analysis procedure originally incorporated in a Windows-based TKUPAV program was completely rewritten in the new ILLISTRS program to reflect the changes in stress adjustment for bonded and unbonded layers and the enhancements of user-friendly features as well as consistency issues. Continuous effort is still underway to modify the existing TKUAPAV program to incorporate the effects of the proposed new design features using Microsoft Visual Basic software (*Microsoft Taiwan Corp., 1997*). These computer programs are available at http://teg.ce.tku.edu.tw.

Table 5. Sensitivity analysis of the effect of second layer on stress reduction (R_5).

Bonded				Unbonded				Unbonded			
E_2=13.78 GPa		h_2 =15.2 cm		E_2 = 0.17 GPa		h_2 =15.2 cm		E_2 =13.78 GPa		h_2 =15.2 cm	
h_2 (cm)	R_5	E_2 (GPa)	R_5	h_2 (cm)	R_5	E_2 (GPa)	R_5	h_2 (cm)	R_5	E_2 (GPa)	R_5
5.1	0.650	1.72	0.737	0	1	0.17	0.999	0.0	1	1.72	0.987
7.6	0.510	3.45	0.579	15.2	0.999	0.34	0.997	7.6	0.987	3.45	0.973
10.2	0.395	6.89	0.398	30.5	0.989	0.69	0.995	15.2	0.902	6.89	0.948
12.7	0.303	13.78	0.229			1.38	0.989	22.9	0.734	13.78	0.902
15.2	0.229	20.67	0.149			2.07	0.984	30.5	0.544	20.67	0.860

Note: Assuming slab thickness h_1 =24.1 cm, slab modulus of elasticity E_1 =27.56 GPa, main landing gear P = 40 kN, dual wheel spacing s = 30.5 cm, and tire pressure p = 689 kPa.

Conclusions and Recommendations

The Corps of Engineers full-scale test pavement data were reanalyzed in this study. Several prediction models proposed by Lee, *et al.* (*1997*) were utilized to estimate the critical edge stress for design. Stress adjustment factors for finite slab width and length were determined and found to be negligible (ranging from 0.964 to 1.0) for the full-scale test pavements.

Since the concept of transformed section was frequently utilized and sometimes misused in the literature to account for the stress reduction due to a bonded or unbonded second layer, a more complete treatment of this concept was presented in this study. By assuming all subbase layers were unbonded, the stress adjustment factor was found to be almost negligible as well (ranging from 0.987 to 1.0). On the other hand, the stress adjustment factor was more pronounced (ranging from 1.0 to 1.248) to account for the discrepancies in the subgrade modulus (k) obtained from Gucbilmez and Yuce (*1995*) against the original pavement design information.

Climatic data close to the test track locations were obtained from the Long-Term

Pavement Performance (LTPP) database in attempts to separate the climatic effects from the fatigue relationship developed earlier. The stress adjustment factor due to effective positive temperature differentials was estimated ranging from 1.0 to 1.241.

The concept of an equivalent stress factor (f_3) and equivalent design factor (EDF) introduced by Lee and Yen (*2001*) was utilized and an alternative structural deterioration model was proposed for future trial design applications A sensitivity analysis of the effect of a bonded or unbonded subbase layer on critical edge stress reduction was conducted to illustrate the potential benefits in adopting newly innovative designs, such as a second bonded layer. Continuous effort is still underway to modify the existing TKUAPAV program to incorporate the aforementioned new design features as part of the proposed design approach.

Furthermore, the effect of load transfer across the joints (currently set to 0.75) and the deficiency of not considering the variability of many factors such as concrete flexural strength, slab thickness, foundation support, slab modulus, etc. as well as the associated inherent biases in determining cumulative fatigue damage in the present FAA design approach should be cautioned and further investigated.

Acknowledgments

This study was sponsored by the National Science Council, Taiwan, the Republic of China. The continuous financial support is very much appreciated.

References

AASHTO (1998). *Supplement to the Guide for Design of Pavement Structures*. American Association of State Highway and Transportation Officials, Washington, D.C.

Darter, M. I., Hall, K. T., and Kuo, C. M. (1995). *Support Under Portland Cement Concrete Pavements*. National Cooperative Highway Research Program, Report 372, Transportation Research Board, National Research Council, Washington, D.C.

Federal Aviation Administration (1995a). *Airport Pavement Design and Evaluation*, Advisory Circular, AC 150/5320-6D.

Federal Aviation Administration (1995b). *Airport Pavement Design for the Boeing 777 Airplane*, Advisory Circular, AC 150/5320-16.

Gucbilmez E., and Yuce, R. (1995). Mechanistic Evaluation of Rigid Airfield Pavements, *Journal of Transportation Engineering*, ASCE, 121(6), 468-475.

Hall, K. T., Darter, M. I., and Kuo, C. M. (1995). "Improved Methods for Selection of k Value for Concrete Pavement Design." *Transportation Research Record 1505*, TRB, National Research Council, Washington, D.C., pp. 128-136.

Kuo C. M. (1994). *Three-Dimensional Finite Element Analysis of Concrete Pavement*, Ph.D. Thesis, University of Illinois, Urbana, Illinois.

Kuo, C. M. (1998). Effective Temperature Differential in Concrete Pavements. *Journal of Transportation Engineering*, ASCE, 124(2), 112-116.

Lee,Y. H., Bair, J. H., Lee, C. T., Yen, S. T., and Lee, Y. M. (1997). "Modified Portland Cement Association Stress Analysis and Thickness Design Procedures." *Transportation Research Record 1568*, Transportation Research Board, Washington, D.C., pp. 77-88.

Lee, Y. H., and Yen, S. T. (2001). "TKUAPAV: A New Thickness Design Program for Rigid Airfield Pavements." In *Advancing Airfield Pavements*, Proceedings, 2001 Airfield Pavement Specialty Conference, ASCE, Edited by W. G. Buttlar and J. E. Naughton III, Held in Chicago, Illinois, August 5-8, pp. 77-86.

Microsoft Taiwan Corp. (1997). *Microsoft Visual Basic. Programmer's Guide and Language Reference*. V.5.0.

NCHRP 1-26 (1990). *Calibrated Mechanistic Structural Analysis Procedures for Pavement*. Vol. 1, Final Report; Vol. 2, Appendices, University of Illinois.

Parker, F., Jr., Barker, W. R., Gunkel, R. C., and Odom, E. C. (1979). *Development of a Structural Design Procedure for Rigid Airport Pavements*, Report No. FAA-RD-77-81, WES-TR-GL-79-4, Government Doc. No. TD 4.509:77-81.

Portland Cement Association (1984). *The Design for Concrete Highway and Street Pavements*. PCA, Skokie, Illinois.

Rollings, R. S., and Witczak, M. W. (1990). Structural Deterioration Model for Rigid Airfield Pavements. *Journal of Transportation Engineering*, ASCE, 116(4), 479-491.

Salsilli-Murua, R. A. (1991). *Calibrated Mechanistic Design Procedure for Jointed Plain Concrete Pavements*. Ph.D. Thesis, University of Illinois, Urbana, Illinois.

Tabatabai-Raissi, A. M. (1977). *Structural Analysis of Concrete Pavement Joints*. Ph.D. Thesis, University of Illinois, Urbana, Illinois.

U.S. Army Corps of Engineers, Waterways Experiment Station (1974). *Comparative Performance of Structural Layers in Pavement Systems*, Vol. 1, Design, Construction, and Behavior Under Traffic of Pavement Test Sections.

Westergaard, H. M. (1948). New Formulas for Stresses in Concrete Pavements of Airfields. *Transactions, American Society of Civil Engineers*, Vol. 113, 425-444.